Shanawanim, M., Paul, D. L., Dumanli, S., & Railton, C. J. (2008). Design of a novel antenna array for MIMO applications. In 3rd International Conference on Information and Communication Technologies: From Theory to Applications (ICTTA 2008), Damascus, Syria. (pp. 1 - 6). Institute of Electrical and Electronics Engineers (IEEE). 10.1109/ICTTA.2008.4530225

Design of a Novel Antenna Array for MIMO Applications

Mazen Shanawani, Dominique Lynda Paul, Sema Dumanli, Chris Railton

Department of Electronic and Electrical Engineering, University of Bristol
Merchant Venturers Building, Woodland Road, Bristol, England, BS8 1UB
{ms6912, d.l.paul, S.Dumanli, Chris.Railton}@bristol.ac.uk

***Abstract*— In spite of the good benefits of using MIMO technology with modern wireless systems, a major problem has arisen from using it with small wireless terminals. When antennas are placed with less than half wavelength apart then mutual coupling occurs. Researchers have found that mutual coupling can affect the performance achieved by multiple antennas which results in a large reduction in channel capacity. In this paper a practical hybrid circuit is designed for a 2x2 MIMO system to confirm a recent theory which states that a decorrelation network can be used with mutually coupled MIMO antennas to improve the performance. The hybrid circuit was tested with stacked patch antennas and performance was evaluated using Cumulative Distribution Function curves on channel capacity at 5.2 GHz. Results show that some improvement was achieved with the hybrid and results can be further improved by some other manipulations.**

I. INTRODUCTION

Multiple Input Multiple Output (MIMO) technology has become widespread in many modern wireless applications. The good reliability and high bit rate it provides makes it most desirable for hand-held devices. However, the minimum spacing requirements [1] makes it difficult to install MIMO antennas on small mobile devices without resulting in mutual coupling. A recent novel theory [2] states that it is possible to restore the performance of MIMO antennas even with very close spacing by using a decorrelation circuit between the receiver and the antenna branches.

In fact, the impact of mutual coupling is quite arguable. Although Dossche's theory [2] has given good results by modelling, some researchers argue that performance will not be restored because the total power collected by all the antennas is similar to that of one antenna [3]. Others argue that the adjacent-antenna setting will impose on the richness of the environment [4]. The impact of noise with mutual coupling has also been studied by Krusevac et al. [5] and gave interesting results.

To investigate the impact of using the decorrelation circuit on MIMO antennas in the real world a hybrid circuit for a 2x2 MIMO system was designed for 5.2 GHz frequency and modelled on computer using Finite Difference Time Domain (FDTD) method. 3D radiation patterns and channel measurements were taken after modelling to calculate the channel capacity.

The organisation of this paper is as follows: Theoretical background for designing the decorrelation network is given in Section II. Section III discusses modelling of the hybrid circuit and the stacked patch antennas which was necessary before the practical design. Actual experiment explanation and the obtained results are given in Section IV. Section V is dedicated to draw conclusions and recommend some experiments for future work.

II. DECORRELATION CIRCUIT DESIGN

To eliminate mutual coupling among antennas a decorrelation circuit may be used [2], [6]. Fig. 1 shows an example of a 4x4 decorrelation circuit proposed for decorrelation in [7]. In Fig. 1, when mutual coupling exists between the input ports 5 though 8, the decorrelation circuit performs decoupling of the signals so that the output signal will have zero mutual coupling. This means that $s_{ij} = 0 \; \forall i, j \in \{1,2,3,4\} : i \neq j$.

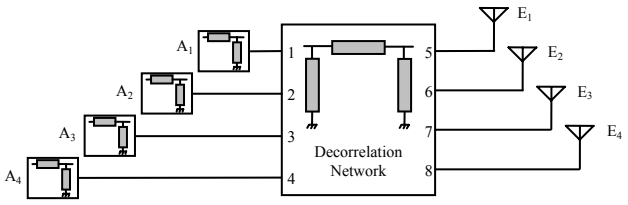

Fig. 1 Schematic decorrelation circuit for 4x4 MIMO antenna array.

In light of this assumption, the decorrelation circuit parameters can be found from the following equations [7]:

$$\sum_i \sum_j P_{ij} q_{m,i} q_{n,j} = 0 \quad \forall m, n \in N : m \neq n \qquad (1)$$

$$\overline{\overline{Q}}.\overline{\overline{Q}}^{H} = I \qquad (2)$$

Where P_{ij} is the energy transmitted from j to i because of mutual coupling, and $q_{i,j}$ are the components of matrix Q. The transmission between the input and output ports is defined by matrix Q[1]. The numbers m and n in Equation 1 represent any two output ports. It is worth noting that equations (1) and (2) hold true for any NxN decorrelation circuit. The circuit also needs matching networks (referred to by A1 …A4 in Fig. 1) at the output to ensure that no reflection on the ports exists. One possible solution is to use two–component (L section) matching networks [8]. In fact, there can be more than one

[1] The transmission matrix Q has the same meaning as S parameters.

solution to the equations above, but the hybrid circuit solution provides a straightforward, frequency-independent, and feasible solution if the elements are symmetrically placed. Therefore, a hybrid circuit was chosen to design the decorrelation circuit.

The hybrid circuit introduces a 180° phase shift between the signals from the two antenna branches [2]. In practice, this hybrid circuit can be fabricated from printed PCB tracks on Duroid 5880 boards. For simplicity, a ring hybrid was chosen for the circuit. The ring circumference can be defined from the desired wavelength, the characteristic impedance is Z_o= 50Ω and the track width can be found from the following equations [9]:

$$\frac{W}{b} = \begin{cases} x & \text{for } \sqrt{\varepsilon_r} Z_o < 120 \\ 0.85 - \sqrt{0.6 - x} & \text{for } \sqrt{\varepsilon_r} Z_o > 120 \end{cases} \quad (3)$$

Where W is the track width and b is the stripline structure height, and x is given by:

$$x = \frac{30\pi}{\sqrt{\varepsilon_r} Z_o} - 0.441 \quad (4)$$

Fig. 2 shows the stripline structure.

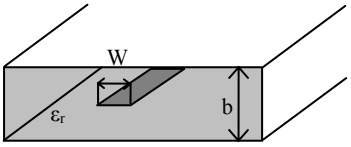

Fig. 2 Cross section in a stripline. The track width is referred to by W and the track height by b.

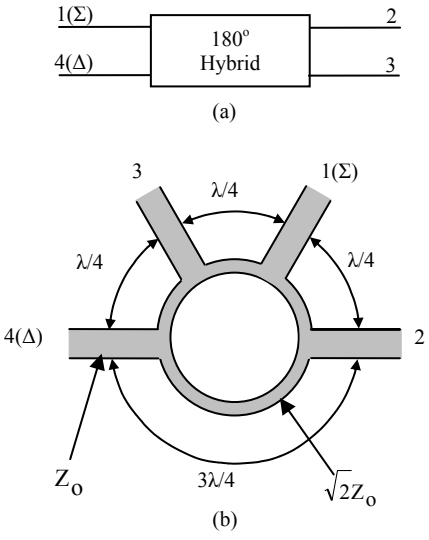

Fig. 3 The schematic (a) and the printed hybrid circuit (b).

Fig. 3(a) shows the schematic hybrid circuit. When the circuit is fed from port 1 (summation) the signal at ports 2 and 3 will have zero phase shift, while feeding from port 4 (subtraction) will result in two equally divided and 180° phase-shifted signals. Fig. 3(b) shows how the hybrid circuit can be implemented with PCB stripline technology [9].

III. Modelling

Out of the available modelling techniques FDTD is preferred over many others because it gives good simulation results with less computer resources compared to other methods such as Transmission Line Method [10]. A program written in the University of Bristol [11] was used to calculate necessary parameters to make sure of the design process. FDTD modelling was performed on both the hybrid circuit and the stack patch antennas to make sure of the design results prior to practical experiment.

The modelling space was divided into small cells to apply the FDTD method on both the hybrid and the pair of stacked patch antennas separately. Fig. 4 shows a plan view of the modelled objects. It can be noticed that the cell sizes are equal in (a), while unequal cells were used in (b). According to [12] this improves the results when the sizes are gradually changed to accurately model fine parts in the modelled object (Eg. Modelling the feed probes, inner connectors, etc).

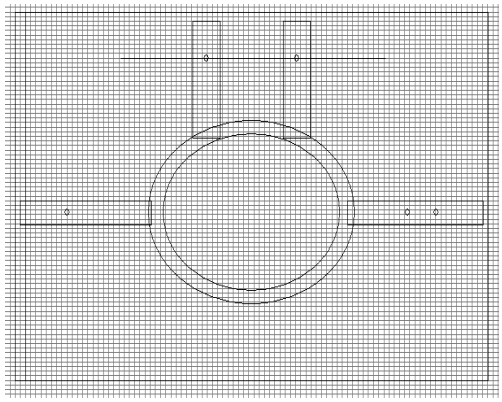

(a)

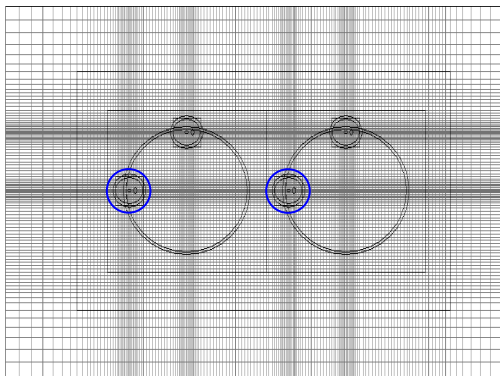

(b)

Fig. 4 A snapshot from the modelling program for (a) the hybrid circuit and (b) the stack patch antennas. It shows that the antennas were adjacently installed so that no clearance exists between them. The primary feeds are circled with blue circles.

S parameters were calculated for both modelled objects based on the results obtained from the FDTD program and using the techniques mentioned in [10]. Fig. 5 and 6 show S parameters for both.

A. *Hybrid Circuit*

Fig. 5 shows the modelling results for the hybrid when feeding from port 4.

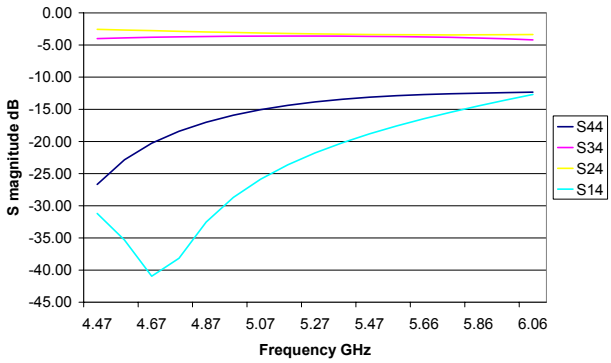

Fig. 5 Simulated magnitude response of S parameters of the hybrid circuit for a frequency range 1-10 GHz when feeding from port 4.

In Fig. 5 S24 and S34 have the value -3 dB which means that the signal is divided equally between ports 2 and 3. Modelling also showed that the phase difference between ports 2 and 3 when feeding from port 4 is 180[o2]. After having good results by modelling, the hybrid circuit was implemented in the University of Bristol laboratory to be tested with the antennas.

B. *The Stacked Patch Antenna*

S parameters were calculated between the two primary feeds (the left hand side feeds in Fig. 4(b)) by modelling. Here, the phase of S parameters was of a minor concern and only magnitudes were plotted in Fig. 6.

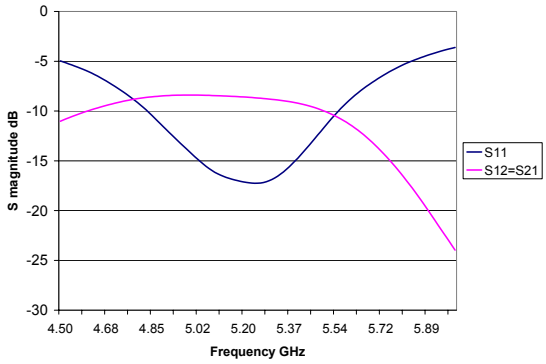

Fig. 6 S parameters magnitudes for mutually coupled stacked patch antennas.

Fig. 6 shows the modelled S parameters between the two primary feeds of the adjacent stack patch antennas. The figure shows the effect of mutual coupling where the signal transmitted from one antenna is partially absorbed by the other antenna. The mutual coupling at f=5.2 GHz is roughly -8 dB which means that about 18% of the transmitted signal from one antenna goes back through the other antenna. Measurements gave similar reflection coefficient curve to that of S11 in Fig. 6 as will be seen in the measurement section.

IV. MEASUREMENTS

To calculate the channel capacity, the stacked patch antennas were mounted on a circular aluminium board. S parameters and radiation pattern measurements were taken in the anechoic chamber with the vector network analyser at the University of Bristol. The indoor channel data was obtained by ray tracing. The channel capacity was calculated using measured data with and without the hybrid circuit. Finally, some options such as rotating the antennas or using the hybrid circuit at both sides were tried. It is worth noting that the same antennas were used for both the sender and the receiver. Fig. 7 shows how the hybrid circuit and the stacked patch antennas were connected.

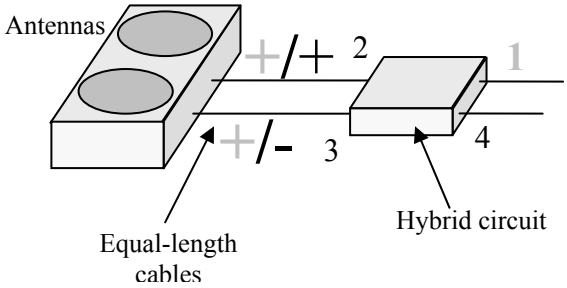

Fig. 7 Connection of the hybrid circuit. This circuit is placed between the stacked patch antennas (represented by the two grey circles), and the MIMO receiver (connected to terminals 1 and 4 of the hybrid circuit).

Equation 5 was used to calculate the maximum channel capacity [4], [14]. It can be used even for imbalanced MIMO systems with M transmitter and N receiver:

$$C = \log_2\left(\det\left(I + \frac{SNR.H.H^T}{M}\right)\right) \text{bit/s} \qquad (5)$$

Where M is the number of the transmit antennas, H is the transmission matrix connecting M transmit antennas to N receive antennas, and $(.)^T$ denotes the conjugate transpose. The components of H can be found from Equation 6 [14]:

$$H_{ij} = \sum_n E_i^R(\theta_n^R, \varphi_n^R).\beta_n.E_j^T(\theta_n^T, \varphi_n^T) \qquad (6)$$

Where H_{ij} is the component of the transmission matrix H between the transmitter j and the receiver i. $E_k^{R(T)}(\theta, \varphi)$ is the electric field value in the far field region of the receive (transmit) array when the array is fed from element k. β is the channel complex path loss.

A. *S parameters*

To measure the impact of mutual coupling and how it was affected by using the hybrid circuit, S parameters were measured for the stacked patch antennas with and without connecting the hybrid circuit. Fig. 8 shows S parameters

[2] The modelling result regarding this point is not shown in this paper.

magnitude for the stacked patch antennas (a) before and (b) after connecting the circuit.

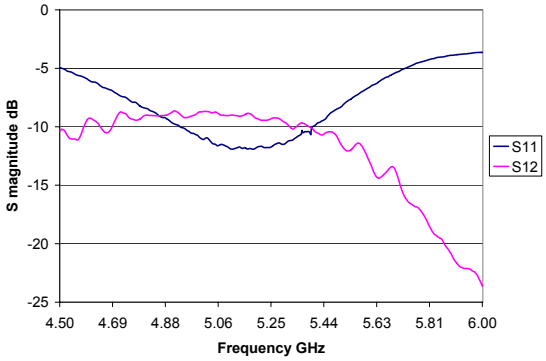

(a)

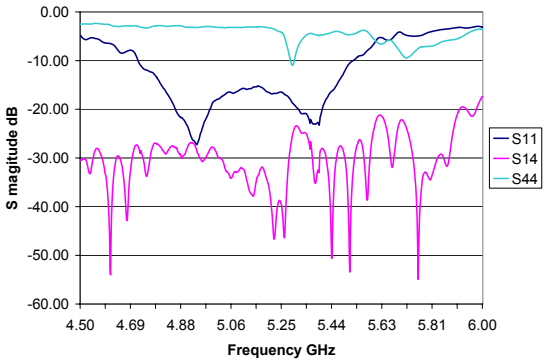

(b)

Fig. 8 Measured S parameters of the stacked patch antennas. (a) Between the two primary feeds as in Fig. 4(b). (b) Between ports 1 and 4 of the hybrid circuit as in Fig. 7.

Fig. 8(a) shows the measured S parameters magnitude between the two primary feeds (Fig. 4(b)). S12 (similar to the simulation results above) is about -8 dB at f=5.2 GHz, while mutual coupling in Fig. 8(b) (between ports 1 and 4 of the hybrid) is roughly -35 dB. This means that the hybrid has decoupled the antennas. The high reflection at port 4 (of the hybrid) is because of the connectors and junction points which could have been improved with better soldering.

B. Radiation Pattern

Measurements were taken in the anechoic chamber. Fig. 9 represents visual representation of the radiation patterns. The use of the hybrid circuit has resulted in very different radiation patterns (c and d) compared to not using the circuit. The impact of mutual coupling has resulted in both antennas having similar patterns when feeding through the left primary feed (a) and the right primary feed (b).

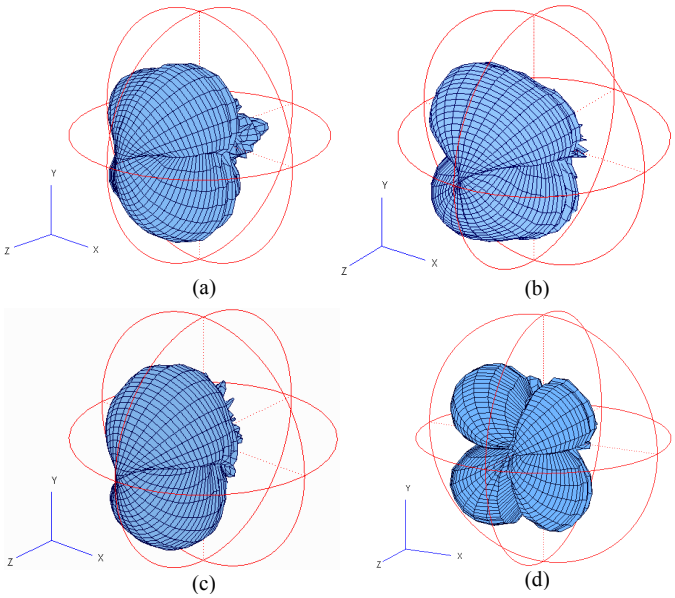

Fig. 9 radiation patterns for stacked patch antennas when the feeding from (a) left primary feed (b) right primary feed (c) though hybrid port 1 (d) through hybrid port 4.

C. Channel Data

Indoor channel data was taken from ray tracing at frequency 5.2 GHz and tried on the collected data using Equation 6. Also, theoretical channel types such as Rayleigh and Rician were tried to calculate channel capacity to evaluate the improvement from using the hybrid.

D. Other Options

To further study the impact of the circuit the hybrid was tried on both channel sides. Also, rotating the antennas was tried to evaluate the improvement from using the hybrid with antenna rotation. Fig. 10 shows the tested configuration.

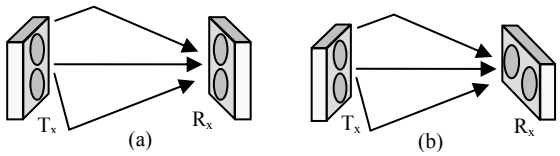

Fig. 10 Positions tried on the receiver antenna. (a) vertical position (b) horizontal position.

V. RESULTS

Results are represented by Cumulative Distribution Function (CDF) curves[3]. Fig. 11 shows that for all channel types there is a slight improvement with the hybrid circuit (decoupled) over using the antennas alone with direct connection to the receiver.

[3] In all plotted curves the chosen Signal to Noise Ratio (SNR) was 20 dB.

A. *Effect of the Hybrid*

Fig. 11 shows the impact of using the hybrid. The figure shows that there is a slight improvement for practical and theoretical channel models.

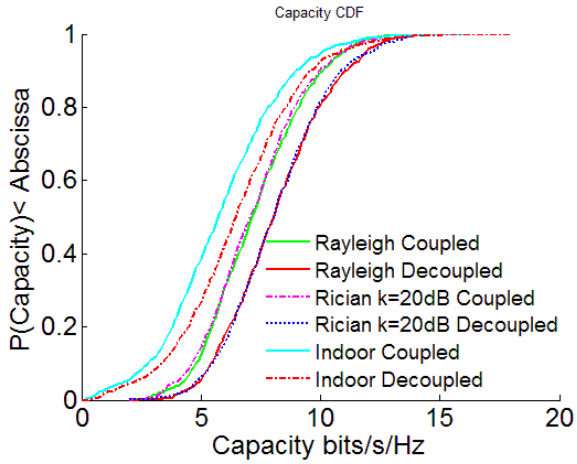

Fig. 11 CDF curves for coupled antennas and decoupled antennas (with hybrid). The figure shows that there is a slight improvement for practical and theoretical channel models.

B. *Using Rotation of the Antennas at one side*

Rotation of the antennas was tried as shown in Fig. 10. Results show slight improvement over the case of using the hybrid alone without rotation. Fig. 12 shows the obtained results.

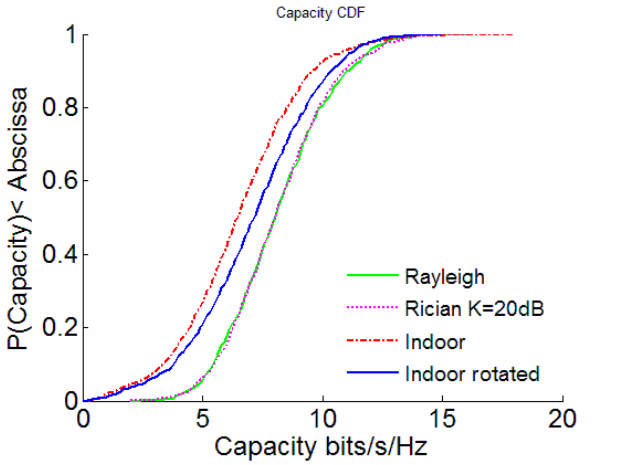

Fig. 12 The impact of rotating the antennas at one channel side. The suffix X'ed refers to rotating the antenna. It shows that with rotation (blue) better performance can be achieved than without rotation (dash-dot red).

C. *Using the Hybrid at the Transmitter and the Receiver*

Fig. 13 shows how the channel capacity is affected by putting the circuit at both the transmitter and the receiver. No improvement is achieved by using the hybrid at both sides. The situation is no different either with or without the rotation mentioned in Fig. 10(b). For example, in Fig. 12 the indoor CDF for using the hybrid *only* at one side (the yellow line) is superimposed over the CDF curve for using the hybrid at both sides (the blue line).

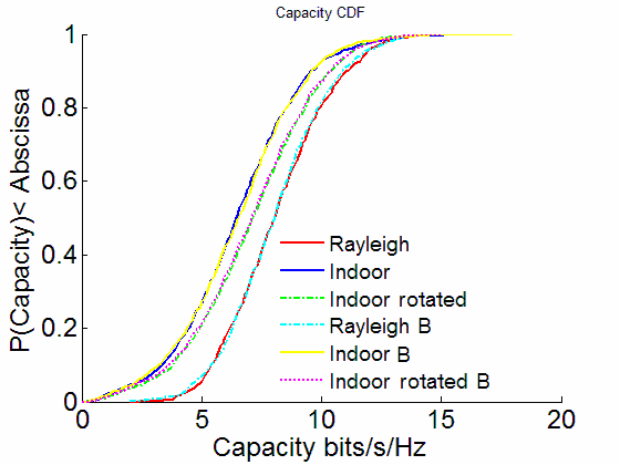

Fig. 13 CDF curves for using the hybrid at both sides. X'ed refers to using the position in Fig. 10(b) and B refers to using the hybrid at both sides.

D. *General Comparison*

A new measurement is taken with widely spaced antennas (where no coupling exists) to benchmark the results with it. Fig. 14 includes CDF curves for widely spaced antennas which are referred to as *apart*. The figure shows that the performance is best with widely spaced antennas for Rayleigh and indoor channels. The figure also shows that degradation (compared to the wide spacing case) occurs with coupled antennas. The use of the hybrid circuit improves the situation even better than the wide spacing case *only* for Rayleigh channels, but offers a middle solution for indoor scenarios. In other words, with the hybrid circuit the system performs better than the coupled case for indoor channels but worse than widely spaced antennas for indoor channels.

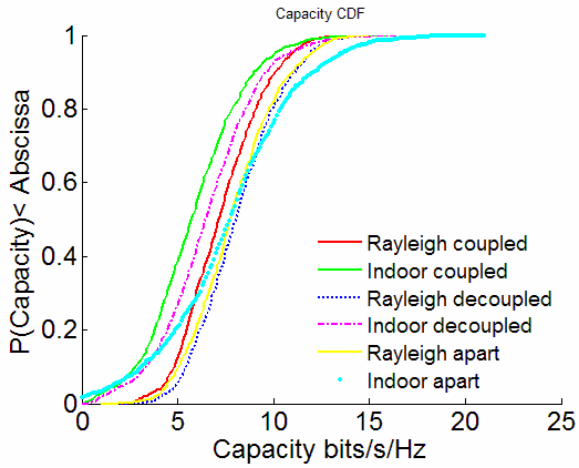

Fig. 14 Performance curves for widely spaced, mutually coupled, and decoupled antennas for Rayleigh and indoor scenarios.

VI. Conclusions And Future Work

A. *Conclusions*

Results of this experiment show that using the hybrid circuit improves the performance of MIMO systems. This result holds true for indoor, Rayleigh or Rician channel scenarios. Assuming that practical channels are a continuum between Rayleigh and Rician channels, this yields to the

conclusion that the hybrid circuit will, in general, improve the performance.

It can be noticed that rotating antennas will further improve the situation (over using the hybrid) for practical channel environments, but no improvement was reported for Rayleigh or Rician channels[4].

B. Future Work

It can be noticed that when SNR=10 dB the improvement is roughly 1 bit/s/Hz. This is only a slight improvement, but it can be further increased by using larger spacing among antennas, using antennas with different radiation patterns to decrease coupling, or using different polarisation (Eg. Primary feed and dual feed for the same example).

In Dossche et al. [2], [15] it is stated that the decorrelation circuit will negatively affect the wideband response. In future research the wideband response is very important as there is a trade-off between the decorrelation level and the bandwidth offered by the decorrelation circuit [2].

With the evolution of modern hybrid designs [16], [17], and [18], future research should focus on integrating newer miniaturised hybrid circuits with the antennas on one board. This is important for modern mobile systems to reduce the space needed on PCB boards.

In [1] it is shown that the maximum transferred information is affected by the matching circuit when the Channel State Information (CSI) is available for the sender. In this research it was assumed that the transmitter is uninformed about the channel status information. Future research may consider using the hybrid with CSI-based MIMO systems.

Finally, the findings in this paper are for a maximum theoretical limit determined by Equation 5. Other future research may focus on the results from using current modulation techniques such as 16-QAM with OFDM.

ACKNOWLEDGEMENT

The authors wish to thank Dr. Geoff Hilton from Bristol University whose program was used to generate the radiation patterns.

Sincere thanks to all the staff in the wireless laboratory in the University of Bristol for their great help and support when taking measurements and supplying ray traced channel data.

The template used to write this paper is a courtesy from Casual Productions.

REFERENCES

[1]. Jensen, M. A. & Wallace, J. W.; (2005); 'Antenna-independent capacity bound of electromagnetic channels'; *Antennas and Propagation Society International Symposium, 2005 IEEE.*

[2]. Dossche, S., Blanch, S. & Romeu, J.; (2005); 'Decorrelation of a closely spaced four element antenna array'; *Antennas and Propagation Society International Symposium, 2005 IEEE.*

[3]. Ozdemir, M. K., Arvas, E. & Arslan, H. (2004) Dynamics of spatial correlation and implications on MIMO systems. *Communications Magazine, IEEE*. [Journal Article]. **Vol. 42**, (6), pp. S14-S19.

[4]. Bolcskei, H., Gesbert, D., Papadias, C. B. & Veen, A. (2006) *Space-Time Wireless Systems*. 1st ed. New York: Cambridge University Press, Chapters. Introduction, 1, 11.

[5]. Krusevac, S., Rapajic, P. & Kennedy, R. A.; (2005); 'Channel capacity of multi-antenna communication systems with closely spaced antenna elements'; *Personal, Indoor and Mobile Radio Communications, 2005. PIMRC 2005. IEEE 16th International Symposium on.*

[6]. Dossche, S., Blanch, S. & Romeu, J. (2004) Optimum antenna matching to minimise signal correlation on a two-port antenna diversity system. *Electronics Letters*. [Journal Article]. **Vol. 40**, (19), pp. 1164-1165.

[7]. Railton, C. (2006) *Modelling a simple 4x4 MIMO system*, Internal report. Electronic and Electrical Engineering Department, University of Bristol.

[8]. Ludwig, R., Bretchko. P.; (2000) *RF Circuit Design Theory and Applications*. New Jersey: Prentice Hall, Chapter. 8.

[9]. Pozar, D. M. (2007) Microwave Engineering. 3rd ed. India: Wiley, Chapters. 3, 4, 7.

[10]. Sheen, D. M., Ali, S. M., Abouzahra, M. D. & Kong, J. A. (1990) Application of the three-dimensional finite-difference time-domain method to the analysis of planar microstrip circuits. *Microwave Theory and Techniques, IEEE Transactions on.* [Journal Article]. **Vol. 38**, (7), pp. 849-857.

[11]. Railton, C. (2001) *A Finite Difference Time Domain Program including Sub-gridding.* 2nd ed.: University of Bristol.

[12]. Railton, C. J., Paul, D. L. & Craddock, I. J. (2003) Analysis of a 17 element conformal array of stacked circular patch elements using an enhanced FDTD approach. *Microwaves, Antennas and Propagation, IEE Proceedings* -. [Journal Article]. **Vol. 150**, (3), pp. 153-158.

[13]. Pal, A., Williams, C., Hilton, G. & Beach, M. (2007) Evaluation of diversity antenna designs using ray tracing, measured radiation patterns, and MIMO channel measurements. *Eurasip Journal on Wireless Communications and Networking.* [Journal Article]. **Vol. 2007**, pp. 58769. Available from: http://dx.doi.org/10.1155/2007/58769.

[14]. Dumanli, S., Tabak, Y., Railton, C., Paul, D. & Hilton, G.; (2006); 'The effect of antenna position and environment on MIMO channel capacity for a 4 element array mounted on a PDA'; *The 9th European Conference on Wireless Technology, 2006.*

[15]. Dossche, S., Blanch, S. & Romeu, J.; (2005); 'Three different ways to decorrelate two closely spaced monopoles for MIMO applications'; *Wireless Communications and Applied Computational Electromagnetics, 2005. IEEE/ACES International Conference on.*

[16]. Weber, J., Volmer, C., Blau, K., Stephan, R. & Hein, M. A. (2006) Miniaturized antenna arrays using decoupling networks with realistic elements. *Microwave Theory and Techniques, IEEE Transactions on.* [Journal Article]. **Vol. 54**, (6), pp. 2733-2740.

[17]. Kuo, J.-T., Chiou, Y.-C. & Wu, J.-S.; (2007); 'Miniaturized Rat Race Coupler with Microstrip-to-CPW Broadside-Coupled Structure and Stepped-Impedance Sections'*; Microwave Symposium, 2007. IEEE/MTT-S International.*

[18]. Hsu, C.-L., Chang, C.-W. & Kuo, J.-T.; (2007); 'Design of Dual-Band Microstrip Rat Race Coupler with Circuit Miniaturization'; *Microwave Symposium, 2007. IEEE/MTT-S International.*

[4] No figure regarding this point is included in this paper.